Analysis of optical emission from high-aluminum AlGaN quantum-well structures

S. Wieczorek,[a] W. W. Chow, S. R. Lee, A. J. Fischer, A. A. Allerman, and M. H. Crawford
Semiconductor Material and Device Sciences Department, Sandia National Laboratories, Albuquerque, New Mexico 87185-0601

(Received 4 February 2004; accepted 21 April 2004; published online 25 May 2004)

The letter presents theoretical analysis of spontaneous emission in AlGaN wurtzite quantum wells. It is found that the combined effects of strain, internal electric field, and many-body Coulomb interactions lead to a significant dependence of optical properties on quantum-well configuration. In particular, the effects of the internal electric field are mitigated for certain Al concentration in the quantum well. Calculations of the emitted photon energy show good agreement with experimental measurements. Presented results are of interest for applications such as ultraviolet light-emitting diodes and lasers. © *2004 American Institute of Physics.* [DOI: 10.1063/1.1763211]

Wide band gap group-III nitride compounds are of great interest as compact sources of short-wavelength radiation. In particular, quantum wells grown with AlGaN alloys are promising candidates for UV light-emitting diodes (LEDs) and lasers,[1–3] with applications in detection of biological agents, medicine, optical memory storage, and solid state lighting. They are usually grown in the wurtzite crystal structure and hence experience strong internal electric fields because of piezoelectric and spontaneous polarization effects.[4–6] The resulting quantum-confined Stark effect (QCSE) together with strong many-body effects result in emission behavior different from those normally observed in typical III–V structures.[7]

In this letter, we analyze the spontaneous emission from AlGaN wurtzite quantum-well structures. After outlining the theoretical approach we discuss theoretical and experimental results for the emission energy. Then, we present spontaneous emission spectra for different carrier densities, and electric field polarizations perpendicular (TE) and parallel (TM) to the quantum-well growth direction. We find significant differences between the spectra for low and high Al concentration in the quantum well. This letter investigates physical effects underlying these dependencies.

We consider a structure composed of uncoupled $Al_xGa_{1-x}N$ quantum wells of width $d=2.8$ nm, $Al_{0.49}Ga_{0.51}N$ barriers of width 5.5 nm, and $Al_{0.53}Ga_{0.47}N$ cladding layers. The unstrained bulk wurtzite material band gap energies are calculated from the empirical formula $E_g=6.2x+3.413(1-x)-0.62x(1-x)$, where the bowing parameter is from Ref. 8. The parameters describing effective masses, crystal-field energy splitting, strain, and piezoelectric and spontaneous polarization fields were obtained using the compositionally weighted averages of the corresponding parameters for AlN and GaN.[5,7,9] The quantum-well band structure calculation involves iterative solution of the **k·p** Hamiltonian and Poisson equation to account for the internal electric field and its screening.

The spontaneous emission spectrum is given by[10]

$$S_{\mathrm{TE(TM)}}(\omega)=\frac{n_b\omega^3}{3\epsilon_0\pi^3c^3\hbar^2\gamma d}\times\sum_{\nu_e,\nu_h}\int_0^\infty dk\,k|\mu_{k;\mathrm{TE(TM)}}^{\nu_e,\nu_h}|^2\times\frac{f_{\nu_e,k}f_{\nu_h,k}}{1-q_k^{\nu_e,\nu_h}}\mathcal{L}(\omega_k^{\nu_e,\nu_h}-\omega),\quad(1)$$

where n_b is the background refractive index, ϵ_0 is the permitivity of free space, c is the speed of light, k is the carrier momentum, $\nu_{e(h)}$ identifies the conduction (valence) quantum well subband, γ is the width of the Lorentzian profile $\mathcal{L}$, $f_{\nu_{e(h)},k}$ is the Fermi–Dirac distribution function for electrons (holes), and $\mu_{k;\mathrm{TE(TM)}}^{\nu_e,\nu_h}$ is the dipole matrix element for the TE (TM) polarization. The many-body Coulomb effects are included within the framework of the Padé approximation. They appear in Eq. (1) via the Coulomb enhancement factor $1/[1-q_k^{\nu_e,\nu_h}]$ and renormalized transition energy $\omega_k^{\nu_e,\nu_h}$.[11] In determining the Fermi–Dirac distribution for electrons and holes we assume fast carrier–carrier scattering and use a common chemical potential for the quantum-well and barrier states.

The quantum-well band gap energy, shown in Fig. 1, is the energy spacing between the lowest energy electron and hole band edges at $k=0$, after including strain, quantum confinement, and QCSE. As shown by the solid curves, the band gap energy increases almost linearly with Al concentration, as the depth of the electron and hole quantum wells decreases. The two solid curves show the case of (i) low carrier density $N_{2D}=10^8$ cm^{-2} and (ii) high carrier density (flatband) where the internal electric field is fully screened. At low carrier densities, the emission energy is approximately the band gap energy minus the quantum-well exciton binding energy (dashed curve in Fig. 1). The quantum-well exciton binding energy is determined from the reduced electron–hole mass, and a form factor of 4 for ideal two-dimensional quantum confinement.[11] It increases slightly with Al concentra-

[a]Electronic mail: smwiecz@sandia.gov

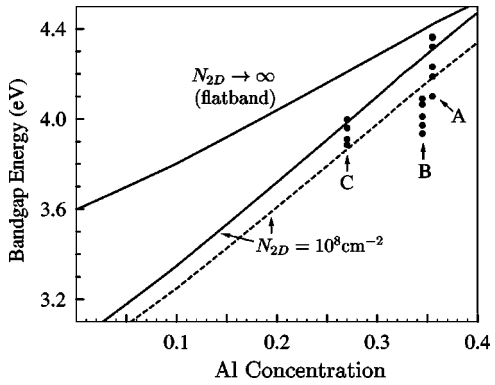

FIG. 1. Calculated band gap energy for $k=0$ vs Al concentration in quantum well (solid curves). The dashed curve and the dots are the calculated and measured emission energies, repectively.

tion and ranges from 0.09 to 0.13 eV. The actual quantum-well exciton binding energy is less, so that emission energy lies between the dashed and solid low-density lines.

In order to experimentally determine the quantum-well transition energies, photoluminescence (PL) measurements were performed on three multiple quantum-well (MQW) samples, which were grown by metalorganic chemical vapor deposition on sapphire substrates. All of the MQWs are five-period structures. For sample A, the MQW contains 5.5 nm $Al_{0.49}Ga_{0.51}N$ barriers and 2.8 nm $Al_{0.35}Ga_{0.65}N$ wells. Samples B and C contain 5.5 nm $Al_{0.40}Ga_{0.60}N$ barriers, with either 2.8 nm $Al_{0.35}Ga_{0.65}N$, or 2.8 nm $Al_{0.27}Ga_{0.73}N$ wells, respectively. The overall structure of sample A was determined by x-ray diffraction (XRD) using radial and transverse scans of reciprocal-space about the (0002), (0004), (10–11), (20–23) and (20–25) reflections. Dynamical diffraction simulations of the symmetric-reflections gave the MQW compositions and thicknesses. The MQW structure of samples B and C were estimated from reactor calibrations using corrections derived from XRD analysis of sample A. The PL measurements were performed using the 325 nm line of a HeCd laser. The system resolution for these measurements is ~0.5 nm. PL measurements, represented by dots in Fig. 1, were performed at multiple positions across a full 50-mm-diam wafer, and the range of PL transition energies is believed to be due to slight epitaxial variations in aluminum concentration and layer thickness.

Theoretical results obtained for the parameters of sample A (dashed curve in Fig. 1) show good agreement with the measured emission energy. The different barrier composition for samples B and C results in a higher theoretical emission energy with average difference of 63 meV from the dashed curve. This places sample C also in good agreement with theory and sample B somewhat below the expected emission energy.

Spontaneous emission spectra for the TE and TM polarizations at two different Al concentrations ($x=0.1$ and $x=0.39$, barrier concentration of 0.49) are depicted in Fig. 2. The spectra reveal strong dependence of the emitted light on the carrier density and quantum-well Al concentration. We label the quantum-well subbands *en* (electron), *hhn* (heavy hole), *lhn* (light hole), and *chn* (crystal-field-split hole), where *n* is the subband quantum number, and note that transitions between *e* and *hh* or *lh* involve only TE polarization, while transitions between *e* and *ch* involve only TM polarization.

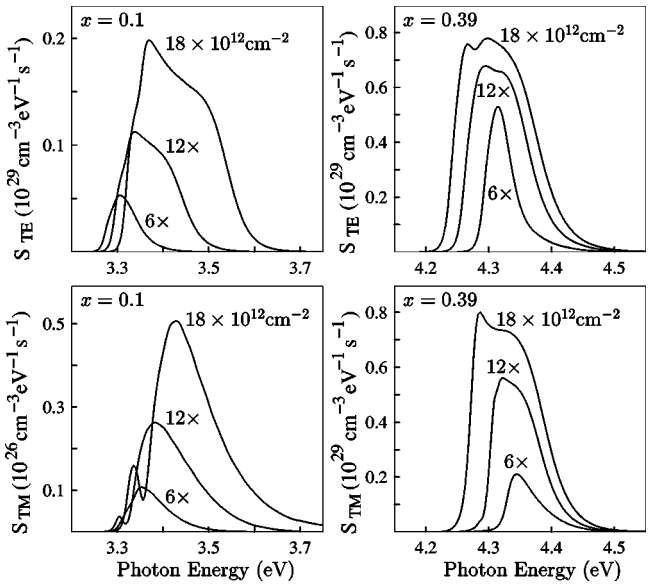

FIG. 2. Spontaneous emission spectra $S(\omega)$ for TE (top) and TM (bottom) polarizations. Al concentrations are $x=0.1$ (first column) and $x=0.39$ (second column). The carrier densities are $N_{2D}=6,12$, and 18×10^{12} cm^{-2}.

For a low Al concentration ($x=0.1$) the quantum well has compressive strain $e=-0.0086$ giving an internal (piezoelectric plus spontaneous polarization) field of 4.26 MV/cm and appreciable electron-hole spatial separation. Injected carriers (i) introduce blueshift due to bandfilling (ii) reduce redshift due to screening of QCSE and (iii) redshift band gap energy due to band gap renormalization. Also, the injected carriers enhance dipole transition matrix elements due to increase of electron–hole wave function overlap. The net effect is a blueshift in the emission peak with increasing excitation [Fig. 2(column 1)] as in InGaN/GaN quantum-well structures.[7] Here, *hh*1 is the lowest hole band in the quantum well. Due to the large separation between *hh*1 and *ch*1, there is little *ch*1 subband population and negligible TM emission.

Increasing Al concentration to $x=0.39$ reduces strain to $e=-0.0022$ and weakens the internal electric field to 1.18 MV/cm. Here, the blueshift due to band filling and screening of the already small QCSE is balanced by the many-body Coulomb interaction induced redshift. The net result is a slight redshift of emission peak with increasing excitation [Fig. 2(column 2)], which is unlike the results from Ref. 7.

Additionally, increasing Al concentration in the quantum well decreases energy separation between *hh*1 and *ch*1, due to changes in the crystal-field energy splitting, to the point where there is a band edge crossover between the two. The precise Al concentration x at crossover depends on strain-induced-shifts. In our case, the crossover occurs at $x \approx 0.315$ and *ch*1 becomes the lowest hole band for $x > 0.315$. This explains a significant (by three orders of magnitude) increase of spontaneous emission into the TM mode as shown in Fig. 2 (bottom row).

The total spontaneous emission rate w_{sp} is obtained by integrating $S(\omega)$ over all transition energies and summing over the TE and TM polarizations. Its dependence on the carrier density and quantum-well Al concentration is summa-

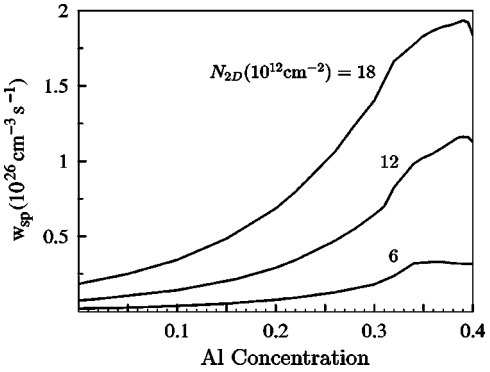

FIG. 3. Total spontaneous emission rate w_{sp} vs Al concentration in the quantum well for different carrier densities N_{2D}.

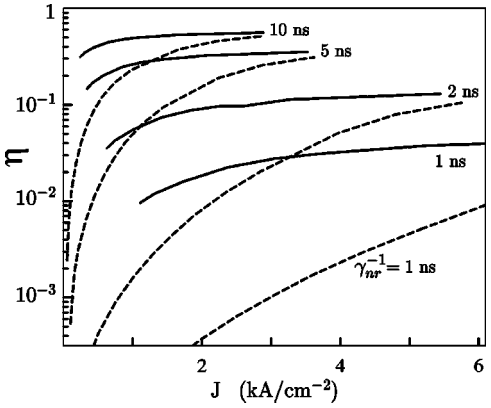

FIG. 4. Efficiency vs current density for different nonradiative carrier decay rates γ_{nr}. Dashed (solid) curves represent Al concentration $x=0.1$ (0.35).

rized in Fig. 3. w_{sp} grows with Al concentration and undergoes a sharp increase at $x\approx 0.3$. This is primarily because the TE mode itself increases abruptly around $x\approx 0.28$, near the crossover where the lowest hole band changes from predominantly *hh*1 to *ch*1. The lighter *z*-direction effective mass of *ch*1 makes the lowest hole band less affected by the internal electric field. As a result, the electron–hole wave function overlap and the dipole matrix element increase (such an effect is also noted for AlGaInN quaternary quantum wells).[12] Concurrently, the TM mode starts rising near $x\approx 0.28$. As *ch*1 shifts to lower energies, eventually becoming the lowest hole band, the *hh*1 and *lh*1 bands shift to higher energies, becoming less populated. Consequently, spontaneous emission into the TE mode starts decreasing at $x\approx 0.35$, so that the total emission rate w_{sp} stops growing near $x=0.38$ [Fig. 3]. With increasing carrier density, the sudden increase in w_{sp} shifts slightly to lower x and the curves flatten. For high carrier densities (not shown in Fig. 3) the internal electric field is fully screened by carriers regardless of x, and w_{sp} shows little dependence on x.

LED efficiency may be defined as $\eta = edw_{sp}/J$ where $J=ed(w_{sp}+\gamma_{nr}N)$ is the injection current density, and γ_{nr} is the nonradiative carrier decay rate. Current leakage is taken into account by assuming equal effective nonradiative decay rates for quantum-well and barrier carrier populations. For the barrier composition considered, the electron and hole confinement potentials are greater than 100 meV even for the highest quantum-well Al concentration of $x=0.4$. As a result, the barrier population remains below 25% of the total density. Figure 4 shows that the efficiency for our AlGaN quantum-well structure may vary appreciably depending on J, γ_{nr}, and Al concentration. At low current density and low x, the appreciable QCSE causes nonradiative recombination due to defects to dominate. As the QCSE is decreased, either by increasing Al concentration or by screening due to injected carriers, the radiative recombination rate increases. Consequently, at low J, η for $x=0.1$ (dashed curves) is much more sensitive to γ_{nr} than η for $x=0.39$ (solid curves). With increasing J the difference between η for the low and the high Al concentration gradually disappears. The efficiency curves for given γ_{nr} saturate when the internal electric field is fully screened by carriers.

In summary, we investigated theoretically and experimentally the ultraviolet emission from wurtzite $Al_xGa_{1-x}N$ quantum wells. Our calculations explain the interplay of strain, quantum confined stark effect, and many-body Coulomb interactions. In particular, we identified an abrupt increase of spontaneous emission rate due to the change in the lowest energy hole band.

This work is partially funded by the United States Department of Energy under Contract No. DE-AC04-94AL85000.

[1] M.R.H. Khan, Y. Koide, H. Itoh, N. Sawaki, and I. Akasaki, Solid State Commun. **60**, 509 (1986).
[2] H. Hirayama, Y. Enomoto, A. Kinoshita, A. Hirata, and Y. Aoyagi, Appl. Phys. Lett. **80**, 37 (2002).
[3] A. Yasan, R. McClintock, K. Mayes, D.H. Kim, P. Kung, and M. Razeghi, Appl. Phys. Lett. **83**, 4083 (2003).
[4] A. Bykhovski, B. Gelmont, and M. Shur, J. Appl. Phys. **74**, 6734 (1993).
[5] J. Wang, J.B. Jeon, Yu.M. Sirenko, and K.W. Kim, IEEE Photonics Technol. Lett. **9**, 728 (1997).
[6] H.S. Kim, J.Y. Lin, H.X. Jiang, W.W. Chow, A. Botchkarev, and H. Morkoc, Appl. Phys. Lett. **76**, 1981 (2000).
[7] W.W. Chow, M. Kira, and S.W. Koch, Phys. Rev. B **60**, 1947 (1999).
[8] S.R. Lee, A.F. Wright, M.H. Crawford, G.A. Petersen, J. Han, and R.M. Biefeld, Appl. Phys. Lett. **74**, 3344 (1999).
[9] O. Ambacher, J. Phys. D **31**, 2653 (1998).
[10] F. Jahnke and S.W. Koch, Phys. Rev. A **52**, 1712 (1995).
[11] H. Haug and S.W. Koch, Phys. Rev. A **39**, 1887 (1989).
[12] W.W. Chow, H.C. Schneider, A.J. Fischer, and A.A. Allerman, Appl. Phys. Lett. **80**, 2451 (2002).